Fermi National Accelerator Laboratory

TM-1554

Linear Beam-Beam Tune Shift Calculations for the TEVATRON Collider

Dave Johnson
Fermi National Accelerator Laboratory
P.O. Box 500, Batavia, Illinois

January 12, 1989

Operated by Universities Research Association Inc. under contract with the United States Department of Energy

Linear Beam-Beam Tune Shift Calculations for the Tevatron Collider

Dave Johnson

January 12, 1989

1.0 Introduction

A realistic estimate of the linear beam-beam tune shift is necessary for the selection of an optimum working point in the tune diagram. Estimates of the beam-beam tune shift using the 'Round Beam Approximation' (RBA) have over estimated the tune shift for the Tevatron. For a hadron machine with unequal lattice functions and beam sizes, an explicit calculation using the beam size at the crossings is required. Calculations for various Tevatron lattices used in Collider operation are presented in Section 2. Comparisons between the RBA and the explicit calculation, for elliptical beams , are presented in Section 3. Section 4 discusses the calculation of the linear tune shift using the program SYNCH. Selection of a working point is discussed in Section 5. The magnitude of the tune shift is influenced by the choice of crossing points in the lattice as determined by the pbar "cogging offsets". Section 6 discusses current cogging procedures and presents results of calculations for tune shifts at various crossing points in the lattice. Finally, Section 7 presents a comparison of early pbar tune measurements with the present linear tune shift calculations.

2.0 Present Calculations

The present calculations are based upon a linearized strong-weak model of the beam-beam interaction.[1] Here, the weak beam is considered as a test particle passing through the strong beam without perturbing the strong beam.

The weak beam receives a transverse kick due to passage through the electromagnetic field of the strong beam. The magnitude of this kick is dependent upon the amount of charge in the strong beam, the transverse dimensions of the strong beam, and the displacement (of the test particles in the weak beam) from the axis of the strong beam. Evans [2] has defined an equivalent magnetic field of the form

$$B_{eq} = \frac{\lambda e(1+\beta^2)}{2\pi\epsilon_0\beta c r}(1 - e^{-r^2/2\sigma^2}) \tag{1}$$

to represent the beam-beam force due to a round gaussian beam, where λ is the charge per unit length in the strong beam bunch, e is the electric charge, $\beta = \frac{v}{c} = 1$, ϵ_0 is the permittivity of free space, c is the speed of light, r is the distance from the axis of the strong beam, and σ is the sigma of the strong beam. To illustrate the magnitude of the field, Figure 1 shows the equivalent field for three values of the strong beam transverse sigma. The values chosen represent a sigma at B0 of 60 microns [for a mini beta lattice], an intermediate value of .1 mm, and a beam sigma of 1 mm, typical of a 150 Gev fixed target lattice. The number of protons per bunch is $6\text{x}10^{10}$ and a bunch length of $\pm$ 1.6 σ_l (with σ_l=.5 m). These are superimposed over a gaussian profile to show the relationship between the transverse distribution of the strong beam and the beam-beam field. It can be seen that the field increases to a maximum value at $\pm$ 1.6 r/σ. The gradient of this field is equivalent to that of a quadrupole which focuses in both planes. For particles in the weak beam undergoing small amplitude oscillations, say $\pm r/2\sigma$, the gradient of the field is linear. For the three cases depicted in figure 1, the maximum gradient (at r=0) has been calculated to be 100 Tesla, 36 Tesla, and .36 Tesla, respectively. These particles receive the maximum tune shift. Particles with larger amplitudes see a smaller gradient, hence are shifted less. This gives rise to the amplitude dependent tune shift which produces a tune spread in the weak beam. Resultant tune distributions of the weak beam have been calculated for an elliptical beam with a gaussian distribution. [3] For the cases calculated in Ref. 3, the peak of the horizontal distribution (for $\sigma_x/\sigma_y = 2$) is approximately 75% of the linear tune shift while the vertical is approximately 60%.

Considering only the linear portion of the field, the maximum linear beam-beam tune shift, ξ, for an elliptical beam with a gaussian distribution, is given by [1,2,4]

$$\xi_{x,y} = \frac{N r_p (1+\beta^2)}{4\pi\beta\gamma(\sigma_x+\sigma_y)} \frac{\beta_{x,y}}{\sigma_{x,y}} \qquad \textit{per crossing} \tag{2}$$

where N is the bunch intensity, r_p is the classical proton radius ($r_p = 1.535\text{x}10^{-18}$ m), $\beta = v/c$ and for the Tevatron equals 1, $\beta_{x,y}$ is the beta function at the crossing, γ is the energy normalization, and $\sigma_{x,y}$ is the "strong" beam size at the crossing. The expression for the beam size is

$$\sigma_{x,y}^2 = \frac{\epsilon_N \beta_{x,y}}{6\pi(\gamma\beta)} + \eta^2 (\frac{\sigma_p}{p})^2 \tag{3}$$

where $\sigma_{x,y}$ is the standard deviation of the transverse beam profile distribution, ϵ_N is the normalized emittance, β is the Courant-Snyder amplitude function, $\gamma\beta$ is a kinematical factor for normalizing the emittance, the 6 in 6π gives a 95% estimate emittance, η is the dispersion function, and σ_p/p is the standard deviation of the momentum distribution.

In order to calculate $\xi_{x,y}$ for the Tevatron, the crossing locations in the lattice of interest must be determined. The crossing locations are dependent on the choice of cogging offset for the pbars. The lattice/cogging offset combinations used in the Tevatron Collider are:

- the fixed target lattice with a 56 bucket cogging offset for the pbars used for injection,
- the fixed target lattice with collision point cogging,
- the 'DEJ'[5] low beta lattice,
- the 1987 100% solution mini beta lattice[6],
- and the 1988 matched mini beta lattice[7].

When the pbars are in the injection cogged configuration the crossings take place about 158 and 683 meters downstream of each straight section. To shift the crossing point to the middle of the CDF detector (in the B0 straight section), the cogging offset is brought to zero; thus the crossings take place at the center of and 525 meters downstream of each straight section. Although collision point cogging has been done at mini-beta and 150 Gev, it is usually done at flattop (900 Gev) with the fixed target lattice. Cogging has generally been avoided in the low beta and mini beta lattices due to the large β_{max} around B0. A discussion of a 150 Gev cogging experiment is given in Section 7. The low beta and both mini beta lattices are evaluated with collision point cogging only.

The lattice functions at each of the 12 crossings are determined using an algorithm to calculate the RF bucket separation and a SYNCH output file (of lattice functions) for each Tevatron lattice studied. The lattice functions for the fixed target lattice, with injection cogging, is shown in Table 1A. The two mini beta lattices, with collision point cogging, are shown in Tables 1B and 1C.

TABLE 1A: FIXED TARGET LATTICE FUNCTIONS

LOC	COG OFF	DISTANCE	β_x	β_y	η_x
E15	28.000	158.068	77.510	37.171	3.290
E35	121.000	683.081	87.339	33.351	1.582
F15	213.500	1205.271	79.309	36.958	3.428
F35	306.500	1730.284	86.251	32.937	1.425
A15	399.000	2252.475	77.506	37.122	3.389
A35	492.000	2777.488	87.039	33.394	1.673
B15	584.500	3299.678	79.192	36.767	3.301
B35	677.500	3824.691	85.793	33.083	1.575
C15	770.000	4346.881	77.460	37.342	3.429
C35	863.000	4871.894	87.689	33.239	1.436
D15	955.500	5394.084	79.235	36.903	3.376
D35	1048.500	5919.097	86.049	32.965	1.681

TABLE 1B: 1988 MINI BETA LATTICE FUNCTIONS

LOC	COG OFF	DISTANCE	β_x	β_y	η_x
E0	0.000	0.000	62.678	65.211	2.628
E28	93.000	525.013	56.353	57.693	2.525
F0	185.500	1047.203	80.583	71.592	4.935
F28	278.500	1572.216	58.057	61.413	2.078
A0	371.000	2094.406	113.117	97.218	5.837
A28	464.000	2619.419	44.092	56.997	3.972
B0	556.500	3141.609	0.688	0.589	0.285
B28	649.500	3666.622	60.385	61.028	8.891
C0	742.000	4188.813	79.252	71.830	-3.025
C28	835.000	4713.825	50.527	59.028	8.078
D0	927.500	5236.016	98.737	92.785	-2.620
D28	1020.500	5761.028	43.098	54.492	5.165

TABLE 1C: 1987 MINI BETA LATTICE FUNCTIONS

LOC	COG OFF	DISTANCE	β_x	β_y	η_x
E0	0.000	0.000	52.821	55.848	1.331
E28	93.000	525.013	20.502	85.044	5.021
F0	185.500	1047.203	43.953	149.661	1.476
F28	278.500	1572.216	81.855	140.437	5.197
A0	371.000	2094.406	140.617	131.789	1.569
A28	464.000	2619.419	125.710	82.063	5.571
B0	556.500	3141.609	0.577	0.615	0.171
B28	649.500	3666.622	78.129	140.372	6.416
C0	742.000	4188.813	141.979	131.549	0.012
C28	835.000	4713.825	126.364	76.604	5.987
D0	927.500	5236.016	241.974	40.738	0.348
D28	1020.500	5761.028	67.433	24.006	5.304

The beam sigmas at the crossings are calculated using equation 3. For comparison with pbar tune measurements, the normalized emittance is taken as the average of the 6 proton bunch's emittance measured by the flying wires.[8] The σ_p/p is obtained from the Sampled Bunch Display [9] measurements of the longitudinal bunch length and the RF voltage. The bunch intensity is the average of the 6 proton bunches. The tune shift parameter at each crossing may then be calculated using equation 2. The total tune shift parameter is the sum of the tune shifts at each crossing.

With 6 proton bunches, each pbar bunch experiences 12 crossings per turn (i.e. 2 times number of proton bunches). If the proton bunches were spaced evenly around the ring, each pbar bunch would experience the same tune shift. However, the proton bunches are spaced using a 185/186 bucket separation (i.e. spacing between p1-p2,p3-p4, and p5-p6 is 186 buckets and the spacing between p2-p3,p4-p5,p6-p1 is 185 buckets). This causes the odd and even numbered pbar bunches to cross the protons at lattice positions separated by .5 bucket (2.8226 meters). This is about a 2% effect in the total tune shift.

During the filling cycle, the beam will sample three or more of the previously described lattices. Since it is of importance to keep the tune shift to a minimum during the transition from injection to the final mini beta lattice, the tune shifts for each of these lattices are calculated. Figures 2 and 3 show the horizontal and vertical tune shifts for each lattice. Here, the vertical emittance is fixed at 20π and the tune shifts are plotted as a function of horizontal emittance. The calculations assume an average bunch intensity of $6\text{x}10^{10}$ and a σ_p/p of $.5\text{x}10^{-3}$ and $.15\text{x}10^{-3}$ for 150 Gev and 900 Gev, respectively. The first observation is that for a typical horizontal emittance of 25π the horizontal tune shift varies by a factor of almost 2 (fig. 2) whereas the vertical tune shift varies only by a factor of 1.3 (fig. 3). The second and probably the most important observation is that the 900 Gev injection cogged configuration has the largest horizontal tune shift while the 150 Gev collision point cogged scenario has the smallest tune shift. The ramifications of this will be further discussed in section 6, on cogging considerations.

A FORTRAN program using these algorithms was written to perform linear tune shift calculations for the 'RBA', the four Tevatron lattices described, and user defined lattice files. The program prompts the user for the type of calculation, lattice, energy, cogging offset, emittances, bunch intensity, and momentum spread. It calculates the tune shift at each crossing and the total tune shift. It will, upon prompt, display cogging offsets, lattice locations, lattice functions, and beam sigmas for each crossing. To access the program, the following command file may be executed:

```
@ADCALC::USR$DISK3:[JOHNSONDE.BBTS]BBTS.COM
```

The output may either be displayed on the terminal or written to a file in the users login area. The output file may be sent to the laser printer in the XGAL computer room upon request. An example of the output is displayed in Figure 4. The first section displays the input data. The second section displays the bucket offsets, the azimuthal distance from Tevatron E0, and the lattice functions at the crossings. The third section displays the beam sigmas and the x/y aspect ratio of the strong beam. The last section displays the tune shift per crossing and accumulated tune shift for the x and y planes.

3.0 Comparison Between 'RBA' and Present Calculations

If we assume

- equal beam sizes for the protons, $\sigma_x = \sigma_y$,
- the crossings occur at locations of zero dispersion, $\eta = 0$, and
- equal horizontal and vertical lattice functions, $\beta_x = \beta_y$,

the expression in equation 2 simplifies to

$$\xi = \frac{3Nr_p}{2\epsilon_N} \qquad \textit{per crossing.} \tag{4}$$

This expression, for the Round Beam Approximation, is independent of the beta function at the crossing, the energy, and gives the same tune shift for both horizontal and vertical $\xi_x = \xi_y$ tunes.

The 'RBA' calculation along with the calculation using equation 2 (for a fixed vertical emittance) as a function of horizontal emittance is shown in Figure 5. Note that below about 30 π the 'RBA' over estimates the tune shift while above about 40 π the 'RBA' predicts a smaller value. The dependence of horizontal tune shift, vertical tune shift, and the 'RBA' on the horizontal emittance are different due the elliptical beam shape at the collision points.

A comparison of the beam size ratios for the lattice/cogging combinations used in the Tevatron Collider indicates that the aspect ratio of the beam may vary from .6 to greater than 3. To compare the beam size ratios for different lattices (with the same cogging offset), a normalized emittance of 20π (for both planes) and a σ_p/p of .5 and .15 (x10^{-3}) is used for 150 and 900 Gev, respectively. The ratios for the 150 Gev and 900 Gev fixed target lattices are shown in Table 2 for both the injection and collision point cogging offsets. The ratios for the fixed target lattice are always greater than unity. When the cogging offset is set to zero (collision point cogging) the ratios are reduced. The low beta lattice has several crossings (A0 thru D0) with a ratio close to unity but the rest of the crossings have ratios close to two. Both the mini beta lattices are not well dispersion matched and have crossings at locations where the dispersion gets as large as 5 meters and in one case approaches 9 meters.

TABLE 2: Beam Size Ratios.

lattice	energy	cogging offset	$(\sigma_x/\sigma_y)_{min}$	$(\sigma_x/\sigma_y)_{max}$
fixed target	150	56	1.8	2.4
fixed target	900	56	1.7	2.0
fixed target	150	0	1.3	2.1
fixed target	900	0	1.2	1.7
Low beta (DEJ)	900	0	1.0	2.6
1987 mini beta	900	0	0.6	3.2
1988 mini beta	900	0	1.2	3.0

If we relax the constraint of equal horizontal and vertical beam sizes and retain the constraint that η is negligible (or equivalently σ_p/p) in the calculation using equation 2, the tune shift is only dependent on the lattice functions (β_x,β_y) at the crossings. The functional form of the horizontal tune shift is closer to that of the 'RBA' approximation, but not identical. Figure 6 shows the 'RBA' and the calculation using the beam size for the case where σ_p/p=0.

For an emittance of 20 π and a bunch intensity of 6x10^{10}, the 'RBA' estimate of the tune shift per crossing is .0022. For six bunches and twelve crossings per turn the total pbar tune shift is .0264. The calculation using equation 2, for the Tevatron gives tune shifts in the range of .013 to .023 depending on the lattice, energy, and cogging offset. Table 3 shows a tune shift comparison between the 'RBA' and the Tevatron lattices used to date. In all cases the above conditions are used. Note that in all cases, the 'RBA' over predicts the tune shift value.

TABLE 3: Tune Shift Comparison of Various Tevatron Lattices

lattice	energy	cogging offset	ξ_x	ξ_y
RBA	-	-	.0264	.0264
fixed target	150	56	.0196	.0169
fixed target	150	0	.0118	.0197
fixed target	900	56	.0233	.0183
fixed target	900	0	.0151	.0219
Low beta (DEJ)	900	0	.0157	.0212
1987 mini beta	900	0	.0131	.0200
1988 mini beta	900	0	.0171	.0217

4.0 SYNCH Calculation

If we equate the tune shift due to a thin quad,

$$\delta\nu = \frac{1}{4\pi}\beta\frac{1}{f} \tag{5}$$

where β is the beta function at the crossing, with equation 2, the focal length of the beam-beam lens is found to be

$$\frac{1}{f} = \frac{2Nr_p}{\gamma\sigma_{x,y}(\sigma_x + \sigma_y)} \qquad \textit{per crossing.} \tag{6}$$

This focal length could range between a few meters upwards to thousands of meters, depending only on the intensity, beam size, and energy. For comparison, the focal length of a Tevatron quad at 900 Gev is about 23.5 meters and the focal length of a Tevatron correction quad powered at 50 Amps (full gradient) at 900 Gev is about 380 meters. As an example of the strength of the beam-beam interaction, lets look at the focal length of the beam-beam interaction at B0 in the "DEJ" low beta lattice. Assume ϵ_h=15π-mm-mr and ϵ_v=20π-mm-mr, we get the sigmas of the beam to be about 60 microns. With 6 E10 protons per bunch, the focal length works out to be about 37.5 meters! If one assumes a bunch length of $\pm$ 1.6σ_l (σ_l=.5 meters), this corresponds to a quad with a gradient of 100 Tesla/meter!

Matrices representing quadrupole lenses focussing in both planes were added to the SYNCH data file at the 12 crossing locations. The focal lengths were calculated assuming a fixed target lattice, an energy of 150 Gev, collision point cogging, horizontal and vertical emittances of 25π and 29π, bunch intensity of 7.5 E10 and a σ_p/p of .5 E-3. These values represent a weak beam-beam interaction with a focal length of about 4.2 km. The tune of the new lattice was calculated and compared to the lattice without the additional nonlinear lenses.

calculation	ξ_x	ξ_y
Eq. 2	.01258	.01850
SYNCH	.01254	.01840
%error	-.3	-.54

The tune shift calculated by SYNCH agrees with that calculated by equation 2 (for the same conditions) to within .6 %.

A comparison of the lattice functions at the crossings between the lattices with and without the nonlinear lenses was made. The beta functions at each crossing show a decrease of less than 1.5% for the lattice with the lenses, except the horizontal beta at B0 which showed a .2% increase. This change in the lattice functions due to the beam-beam interaction is referred to as the dynamic beta effect[1]. If the emittances were reduced or the bunch intensity increased, this dynamic beta effect would be more pronounced. Chao[1] points out that the luminosity should scale as the ratio of the unperturbed to the perturbed beta functions, β/β^*, at the crossings. Additionally, Chao points out that the weak beam is most unstable if the tune advance, $\psi/2\pi$, between crossings is just below .5 and most stable if just above .5. For the injection cogged fixed target lattice, the tune advance between the crossings in the unperturbed lattice is in the range of 1.54 to 1.69 which is slightly above a tune of (modulo) .5.

5.0 Working Point Considerations

To date the working point for the Tevatron has been between the $2/5^{ths}$ and the $3/7^{ths}$ resonances. Both of these resonances lead to beam loss or emittance growth during proton only stores. The next higher resonance that lies between these are the 12^{th} order resonances. We have typically chosen a working point for the proton tunes in the range of $\nu_x = .410$ to .415 and $\nu_y = .405$ to .410 which places the tunes about .005 units below the coupling diagonal. The beam-beam interaction is expected to excite even order resonances for head-on collisions.[10] The 10^{th} order resonances have been shown to reduce the pbar lifetime at the CERN as reported by Evans.[2,11] Non-zero dispersion at the crossings can drive odd order resonances.[2] Again, Evans[2] reports that the 7^{th} order resonances were "extremely destructive" to the pbar lifetime. These statements would seem to say that the working area should be free of resonance lines. With large proton and pbar intensities, this is a difficult task.

If we assume a working point for the protons of $\nu_{x0} = .410$ and $\nu_{y0} = .405$, the maximum pbar tune, $\nu_{x,y} + \xi_{x,y}$, may be plotted for each of the lattice/cogging combinations in Table 3. It should be noted that these tune values assume zero coupling. Figure 7 shows the working diagram[12] between the 5^{th} and 9^{th} order resonances. Point 1 represents a base tune for protons in the absence of any pbars. As the pbars are injected, the small amplitude pbars are shifted to the point 2 which corresponds to the 150 Gev fixed target injection cogged lattice. Ramping to flattop shifts the maximum pbar tune to point 3, still with injection cogging. Upon collision point cogging the maximum pbar shift is indicated by point 4. The low beta and the 100% 1987 mini beta are indicated by points 5 and 6. Points A and B are the 150 Gev fixed target collision point cogged lattice and the 1988 mini beta lattice. Also shown is the prediction of the 'RBA'.

It should be noted that the maximum pbar tune shifts for the cases in table 3 are clustered around the 7^{th} order resonances. To avoid the $\nu_x = 3/7^{ths}$ and maintain the .005 units below the diagonal, the maximum tune shift, $\xi_{x,y}$, allowed would be .0185 in each plane.

In order to provide a larger working area, alternate working points above the 13^{th} order resonances and above the integer are currently being discussed.

6.0 Cogging Considerations

The current Tevatron injection scheme fills the Tevatron with 6 proton bunches spaced around the ring and then injects a pbar bunch between each pair of proton bunches. The separation between proton bunches is about 3.5 μsec or about 1.05 kilometers. This requires the pbar injection kicker to be fast enough to inject pbars without effecting the neighboring proton bunches. Since the decay time of the kicker is longer than the rise time, the pbars are injected about 1.05 μsec after each proton bunch which corresponds to a 56 bucket offset. Previous pbar kicker timing experiments show that the pbar injection cogging offset cannot be moved more than +/- 2 or 3 buckets without effecting the neighboring protons.[13]

A scan of the linear beam-beam tune shift was made for various crossing points in the Tevatron lattice to show the relationship between the tune shift and the lattice parameters, β and η. This scan was accomplished by varying the cogging offset for the A1 (pbar) bunch from 0 to 186 buckets. This shifts the relative location of the A1 bunch to all 6 proton bunches and shifts the 12 collision points between the A1 bunch and the 6 proton bunches. As the offset is changed through one sector (186 buckets) this maps out the tune shift through the entire Tevatron lattice. This procedure was used to map out five Tevatron lattices used during this run.

The first lattice of interest is the Tevatron 150 Gev fixed target lattice used during injection. This is shown in Figure 8. The current cogging offset of 56 buckets is shown on the diagram. With this cogging offset the crossings take place between the 15 and 16 location and between the 35 and 36 locations in all six sectors. The average of the horizontal and vertical tune shifts is .020. Two other potential offsets are indicated. One for 79 buckets and the other as a 97 bucket offset. These give average tune shifts of .0133 and .0124, respectively. Another option is to perform collision point cogging at this energy to give a 0 bucket offset and an average tune shift of .0157. This will reduce the horizontal tune shift while not effecting the vertical to a great extent. The oscillatory nature of the horizontal tune shift is due to the variation of β and η around the ring. The minimum horizontal value corresponds to crossing points just upstream of the 28 location and downstream of the 29 location where η is large, about 4 to 5 meters.

Once all bunches are in the Tevatron, they are ramped to 900 Gev using the fixed target lattice. Figure 9 shows a general increase in the average tune shift of about .004 for 900 Gev fixed target lattice over the 150 Gev fixed target lattice. Specifically, average tune shift for the 56 bucket injection cogging offset at 900 Gev increases to .0235. This condition gives rise to the largest tune shift of any lattice/cogging combination (fig.2) and should probably be avoided. Once at flattop, the pbars are collision point cogged which means that they are shifted by -56 buckets to bring the crossings to the straight sections and mid way between the straight sections, i.e. between the 28 and 29 locations.

It is not clear whether any emittance dilution or beam loss could be prevented by either performing collision point cogging at 150 Gev prior to ramping or using the 97 bucket offset during acceleration.

Figures 10 through 12 show the cogging offset for the "DEJ" low beta lattice as well as the 1987 100% mini beta lattice solution and the 1988 matched mini beta solution. The 1988 solution generally shows a lower tune shift due to the increased dispersion around the ring.

7.0 Comparisons with Pbar Tune Measurement

Until recently, the measurement of the pbar tunes was not possible. Much work has gone into setting up and tuning the Schottky detectors and electronics for rejecting the proton signal and only processing the signal from the pbars.[14]

Pbar tune measurements were made about 20 hrs into store 1578. The results of these measurements give maximum tune spreads of $\Delta\nu_x = .008$ and $\Delta\nu_y = .007$.[15] As the bunch intensity of the pbars is increased, the protons will also be shifted upward in tune. For equal emittances (of protons and pbars), the magnitude of the proton tune shift is just the ratio of bunch intensities. The beam emittances and intensities for both protons and pbars were recorded during the same time. These were used to calculate a tune shift for both the protons and pbars. The protons were shifted up by .0059 and .0061 for the horizontal and vertical, respectively. The pbars were shifted by .0132 and .0138. The measurements show the relative tune shift between the pbars and protons, so the difference between the shifts are calculated to be $\Delta\nu_x$=.0073 and $\Delta\nu_y$=.0077, from the linear calculation.

An early attempt [store 1618] to perform collision point cogging at 150 Gev was seen to reduce the horizontal pbar tune shift. The tune spectra from the horizontal Schottky plates (looking at both proton and pbar tunes) before and after the cogging are shown in Figure 13A [16] while the spectra from the vertical Schottky plates (looking only at the proton tune) are shown in Figure 13B. In each figure, the upper spectrum was taken before collision point cogging while the lower spectrum was after collision point cogging. The $2/5^{ths}$ and the $3/7^{ths}$ resonance lines are indicated in each figure as dashed and dot- dashed lines.

Figure 13A clearly shows a shift in the right hand edge of the spectra. The lower spectrum, representing collision point cogging clearly has a smaller tune shift. A rough measurement of the magnitude of the shift shows a difference, $\Delta\nu_{max}$, of -.0062 $\pm$ .002. The uncertainty in this number represents how well the edge of the tune distribution can be measured. The vertical before and after spectra, in Figure 13B, does not show this shift in the upper edge of the tune spectra. A large peak, at a tune of .4273, is seen in the after cogging spectra. This is presumably a tune line associated with a π mode coherent bunch oscillation. [17]

Further quantitative information from these spectra is difficult due to the presence of horizontal-vertical coupling and the presence of 60 Hz noise in the spectra. Since these data were taken additional work has been done on the pbar measurement system.[17]

If one looks at the spectra from the pbar output of a Schottky detector and assumes that the right hand edge of the spectra corresponds to the maximum tune of the pbars, ν_{max}, and the base proton tune, ν_0, is known (from a proton only store) a maximum tune shift could be measured. This would be given by:

$$\xi = \nu_{max} - \nu_0. \tag{7}$$

If the base proton tune is not known, a comparison of spectra between two different cogging offsets should yield the difference in pbar tune shifts between the two cogging offsets. This is, in effect, a measure of the difference in the lattice functions at the different crossings. Taking the tune difference of the right hand edge of the horizontal tune spectra before and after cogging as a measure of the maximum pbar tunes, the relative difference between cogging offsets may be inferred from equation 7:

$$\xi_{after} - \xi_{before} = (\nu_{max} - \nu_0)_{after} - (\nu_{max} - \nu_0)_{before}$$

$$\Delta\xi = \Delta\nu_{max} \tag{8}$$

Using the measured bunch intensities and emittances for both the protons and pbars, the linear tune shift was calculated for the 150 Gev injection cogged lattice and the 150 Gev collision point cogged lattice. The relative tune shift between the protons and pbars are tabulated below with the bottom line being the expected shift in the maximum pbar tune, $\Delta\nu_{max}$, between the different cogging offsets.

cogging offset	ξ_x	ξ_y
coll pt.	.0054	.0099
inj cog.	.0123	.0108
$\Delta\xi$	-.0069	-.0009

This $\Delta\xi_x$ is to be compared with the $\Delta\nu_x$ in Figure 13A.

Large losses during the low beta squeeze persuaded us to revert back to collision point cogging at flattop until the losses were understood and better pbar tune measurements were possible.

8.0 Conclusions

For the Tevatron lattices studied (using typical beam emittances) the 'RBA' always over predicts the linear calculation. The SYNCH calculations using non-linear lenses due to the beam-beam interaction agree with those using eq. 2. For the injection cogged fixed target lattice, the dynamic beta effect is small. The comparisons between the linear tune shift calculations and early pbar tune measurements are encouraging, at least giving order of magnitude results. Further measurements are needed to test the calculation of the maximum linear tune shift. The results of the cogging experiment seem to agree in sign and order of magnitude to the predictions of the linear tune shift calculations. This approach appears promising as a technique for comparisons with the linear tune shift predictions. In the absence of beam separators and as the proton and pbar intensities are increased, the present working area will not be able to contain both protons and pbars in a resonance free area. This will necessitate the search for a new working point.

9.0 References

1. A. W. Chao, Beam-Beam Instability, Proceedings of 1983 Accelerator Summer School, pages 201-242.
2. L. R. Evans, The Beam-Beam Interaction, CERN SPS/83-38.
3. E. Keil, Non-Linear Space Charge Effects I, CERN/ISR-TH/72-7.
4. E. Keil, Beam-Beam Interactions in p-p Storage Rings, CERN 77-13, p. 314.
5. D. E. Johnson, Tevatron B0 Low Beta Tuning Report, TM-1106, May 1982.
6. Mini beta solution by C. Ankenbrandt, 1987.
7. Matched Mini Beta solution by D. Finley, 1988.
8. J. C. Gannon, et.al., 'Flying Wires at Fermilab', abstract submitted to 1989 Particle Accelerator Conference.
9. C. Moore, et.al., 'Single-Bunch Intensity Monitoring System Using an Improved Wall Current Monitor', abstract submitted to 1989 Particle Accelerator Conference.
10. W. T. Weng, Space Charge Effects-Tune Shifts and Resonances, AIP Proceedings No. 153, (1984/1985 Accelerator Summer School), pages 378-388.
11. L. R. Evans and J. Gareyte, Beam-Beam Effects, CERN SPS/86-8
12. DI-3000 graphics program for the display of the tune diagram was developed by Y. Chao
13. J. Gannon private communication.
14. Work done by instrumentation group.
15. Measurements made by G. Jackson, Sept. 1988.
16. Application program for tune display was developed by G. Jackson.
17. G. Jackson private communication.

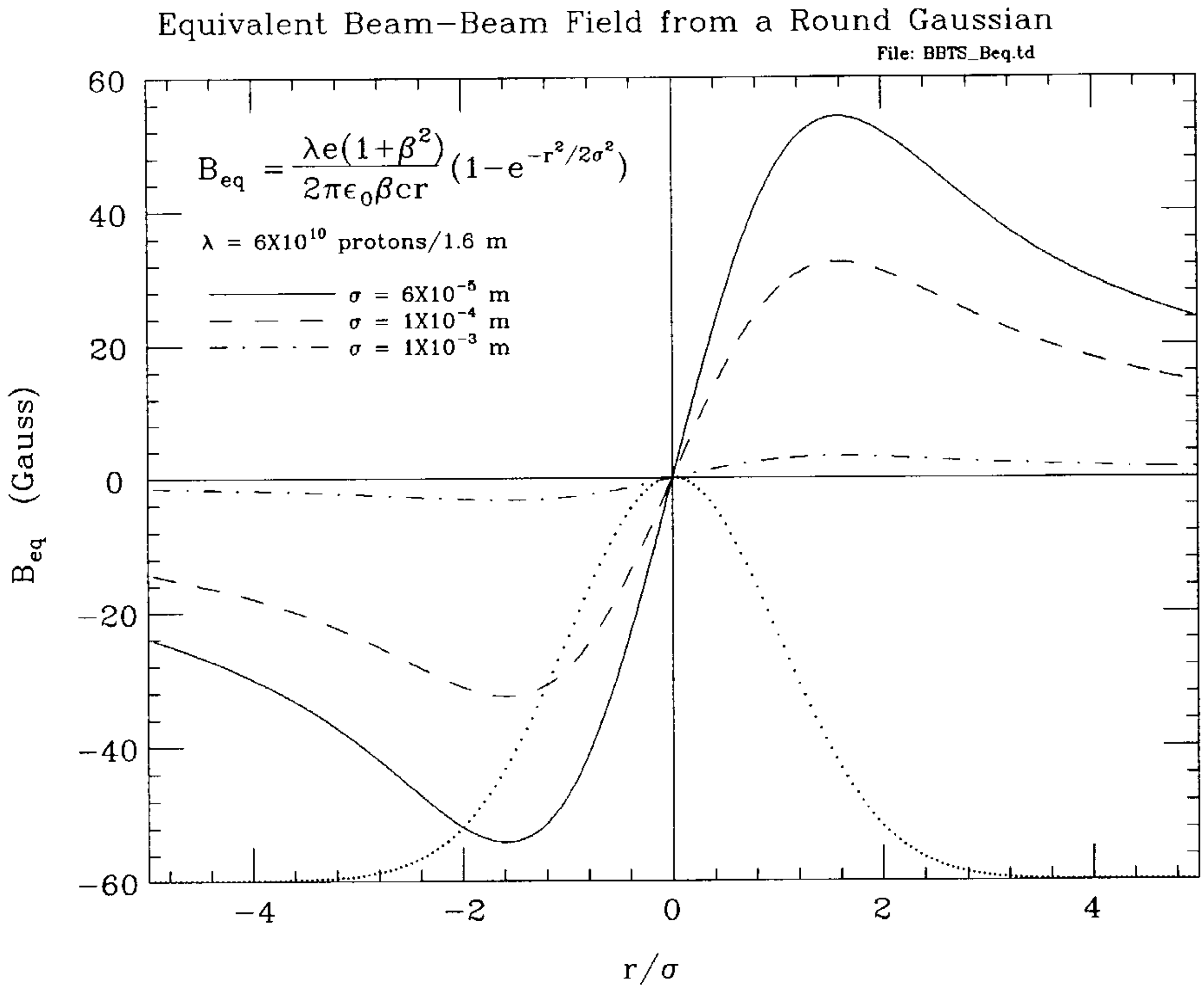

Equivalent Beam−Beam Field from a Round Gaussian
File: BBTS_Beq.td
$B_{eq} = \frac{\lambda e(1+\beta^2)}{2\pi\epsilon_0 \beta c r}(1-e^{-r^2/2\sigma^2})$
λ = 6X10^{10} protons/1.6 m
σ = 6X10^{-5} m
σ = 1X10^{-4} m
σ = 1X10^{-3} m
60
40
20
0
−20
−40
−60
B_{eq} (Gauss)
−4
−2
0
2
4
r/σ

FIGURE 1

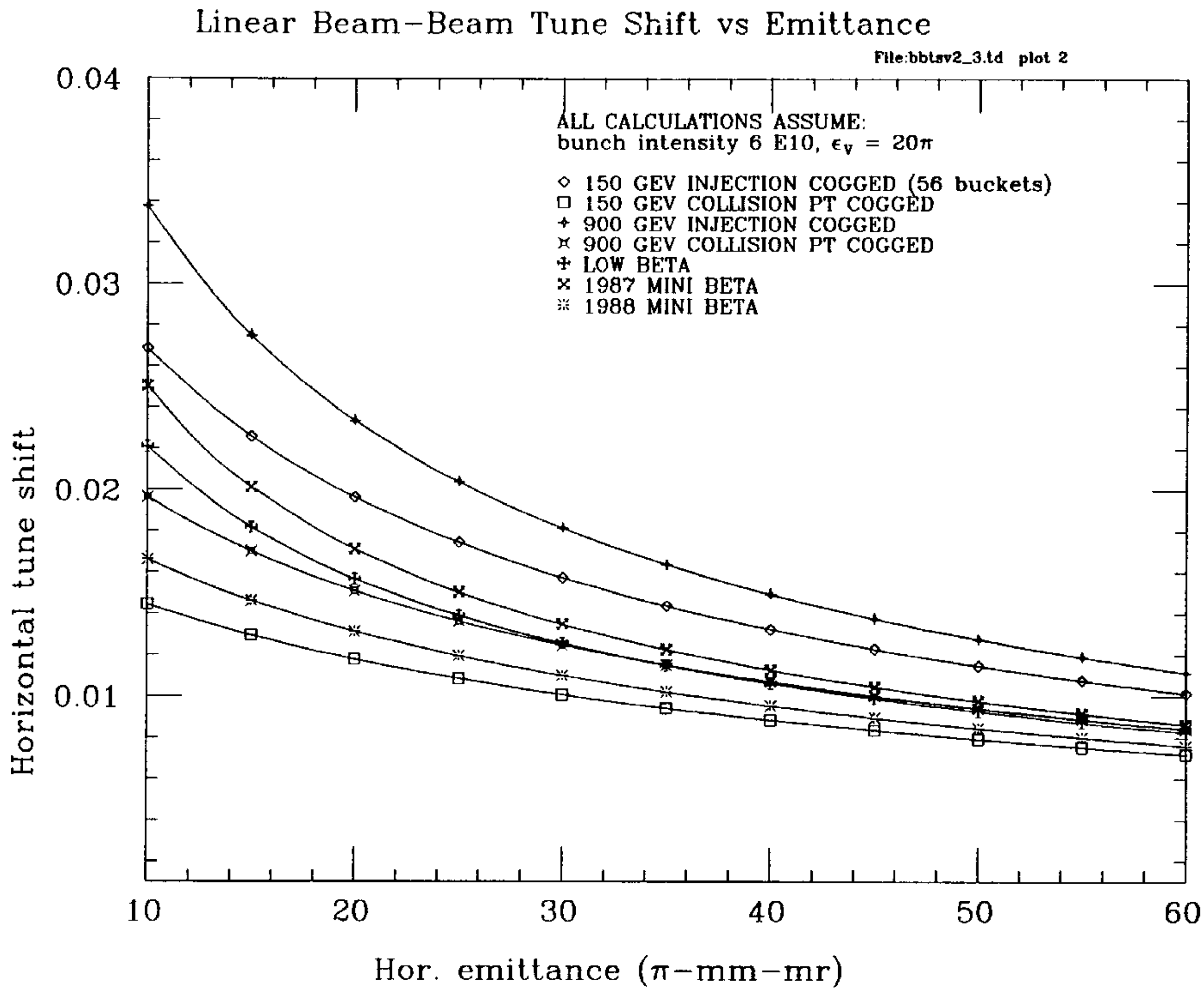
Linear Beam-Beam Tune Shift vs Emittance
File:bbtsv2_3.td plot 2
ALL CALCULATIONS ASSUME:
bunch intensity 6 E10, $\epsilon_v = 20\pi$
◇ 150 GEV INJECTION COGGED (56 buckets)
□ 150 GEV COLLISION PT COGGED
+ 900 GEV INJECTION COGGED
900 GEV COLLISION PT COGGED
LOW BETA
1987 MINI BETA
1988 MINI BETA
0.04
0.03
0.02
0.01
Horizontal tune shift
10
20
30
40
50
60
Hor. emittance (π-mm-mr)

FIGURE 2

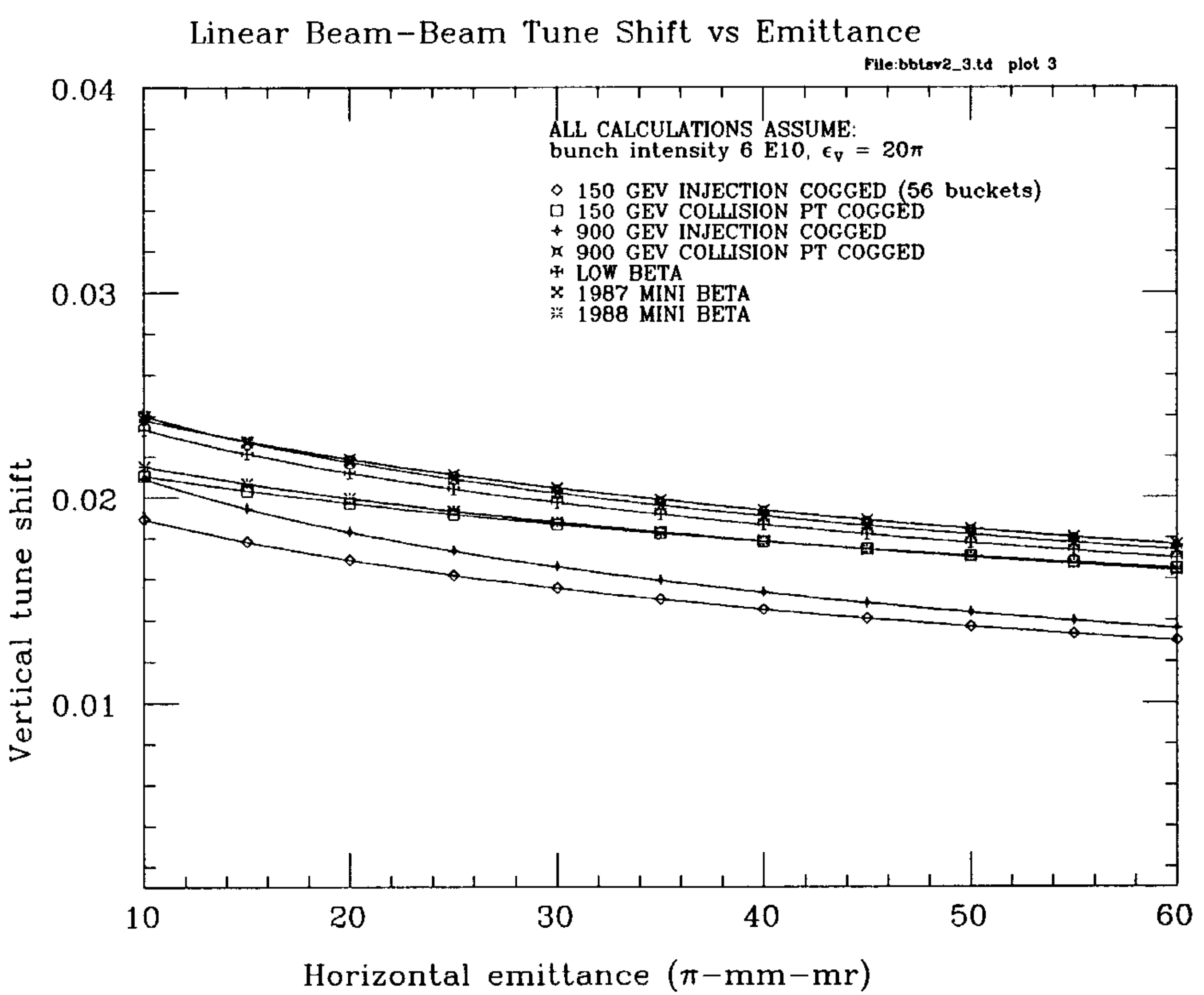

Linear Beam-Beam Tune Shift vs Emittance
File:bbtsv2_3.td plot 3
ALL CALCULATIONS ASSUME:
bunch intensity 6 E10, $\epsilon_V = 20\pi$
150 GEV INJECTION COGGED (56 buckets)
150 GEV COLLISION PT COGGED
900 GEV INJECTION COGGED
900 GEV COLLISION PT COGGED
LOW BETA
1987 MINI BETA
1988 MINI BETA
Vertical tune shift
0.04
0.03
0.02
0.01
10
20
30
40
50
60
Horizontal emittance (π-mm-mr)

FIGURE 3

```
lattice is 1987 minibeta
cogging offset for A1   0.0000000E+00
energy    900.0000
hor emit.     12.40000      ver emit.    17.90000
intensity     5.250000      dpop     0.1200000
 crossing      bckt        dist       betax       betay        etax
        1      0.000       0.000      52.821      55.848       1.331
        2     93.000     525.013      20.502      85.044       5.021
        3    185.500    1047.203      43.953     149.661       1.476
        4    278.500    1572.216      81.855     140.437       5.197
        5    371.000    2094.406     140.617     131.789       1.569
        6    464.000    2619.419     125.710      82.063       5.571
        7    556.500    3141.609       0.577       0.615       0.171
        8    649.500    3666.622      78.129     140.372       6.416
        9    742.000    4188.813     141.979     131.549       0.012
       10    835.000    4713.825     126.364      76.604       5.987
       11    927.500    5236.016     241.974      40.738       0.348
       12   1020.500    5761.028      67.433      24.006       5.304
  crossing       sigx           sigy          sigx/sigy
         1  3.7306230E-04  4.1649479E-04  0.8957190
         2  6.3806068E-04  5.1395601E-04   1.241469
         3  3.5488841E-04  6.8180281E-04  0.5205147
         4  7.5169274E-04  6.6045905E-04   1.138137
         5  5.8137247E-04  6.3980045E-04  0.9086778
         6  8.4698683E-04  5.0487003E-04   1.677633
         7  4.0749750E-05  4.3707718E-05  0.9323239
         8  8.7223650E-04  6.6030648E-04   1.320957
         9  5.5271626E-04  6.3921692E-04  0.8646771
        10  8.8774954E-04  4.8778762E-04   1.819951
        11  7.2277151E-04  3.5571860E-04   2.031863
        12  7.4172480E-04  2.7306320E-04   2.716312
 IP xtuns(ip)      xtunst      ytuns(ip)      ytunst
  1  .23958E-02   .23958E-02   .22690E-02   .22690E-02
  2  .37265E-03   .27685E-02   .19190E-02   .41880E-02
  3  .15961E-02   .43646E-02   .28289E-02   .70169E-02
  4  .10302E-02   .53948E-02   .20117E-02   .90286E-02
  5  .26462E-02   .80410E-02   .22536E-02   .11282E-01
  6  .14668E-02   .95078E-02   .16064E-02   .12889E-01
  7  .22394E-02   .11747E-01   .22260E-02   .15115E-01
  8  .78087E-03   .12528E-01   .18533E-02   .16968E-01
  9  .28793E-02   .15407E-01   .23068E-02   .19275E-01
 10  .13825E-02   .16790E-01   .15253E-02   .20800E-01
 11  .41473E-02   .20937E-01   .14187E-02   .22219E-01
 12  .11969E-02   .22134E-01   .11574E-02   .23376E-01
```

FIGURE 4

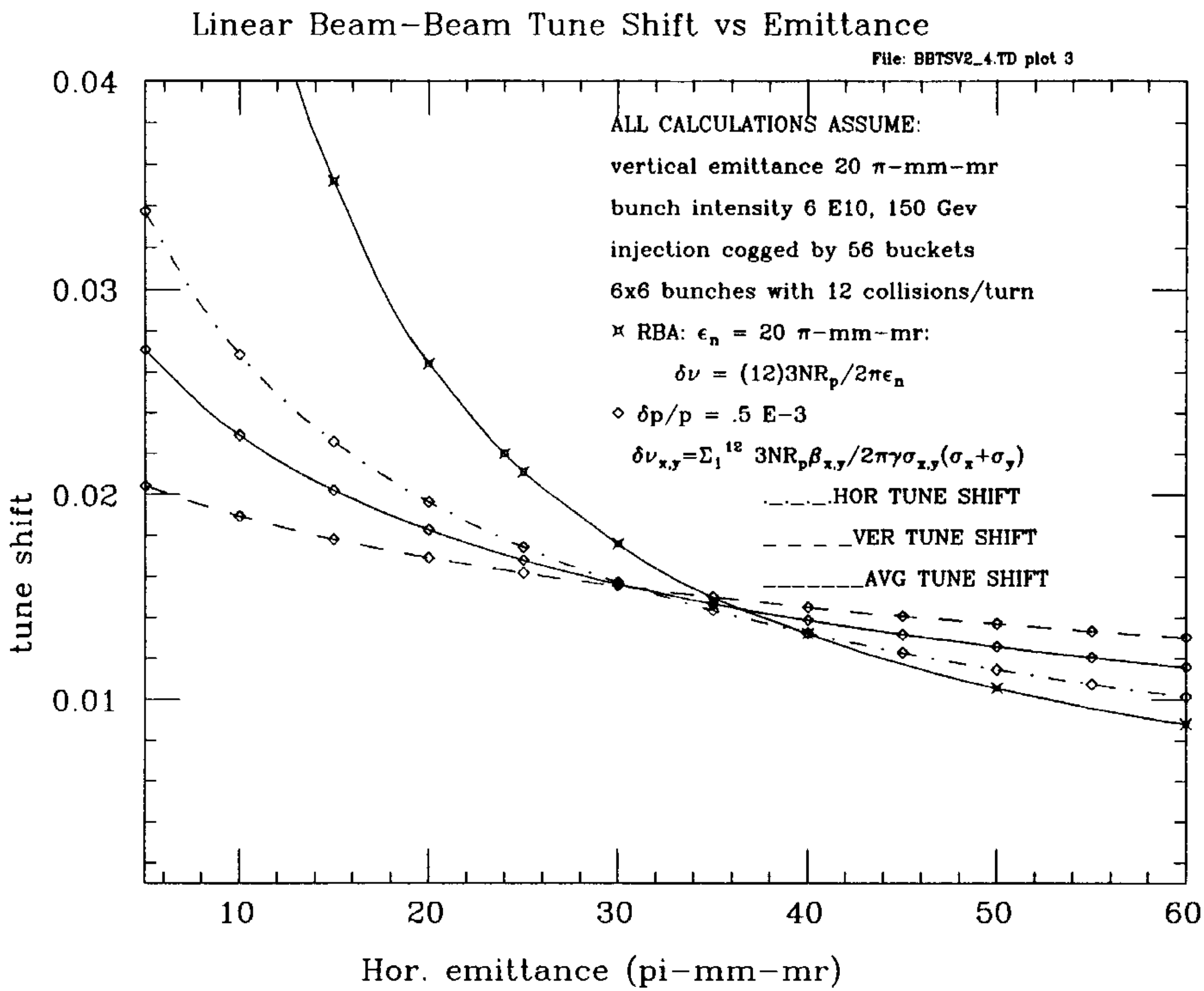

Linear Beam-Beam Tune Shift vs Emittance
File: BBTSV2_4.TD plot 3
ALL CALCULATIONS ASSUME:
vertical emittance 20 π-mm-mr
bunch intensity 6 E10, 150 Gev
injection cogged by 56 buckets
6x6 bunches with 12 collisions/turn
RBA: ϵ_n = 20 π-mm-mr:
$\delta\nu = (12)3NR_p/2\pi\epsilon_n$
$\delta p/p$ = .5 E-3
$\delta\nu_{x,y}=\Sigma_1^{12}\ 3NR_p\beta_{x,y}/2\pi\gamma\sigma_{x,y}(\sigma_x+\sigma_y)$
HOR TUNE SHIFT
VER TUNE SHIFT
AVG TUNE SHIFT
0.04
0.03
0.02
0.01
tune shift
10
20
30
40
50
60
Hor. emittance (pi-mm-mr)

FIGURE 5

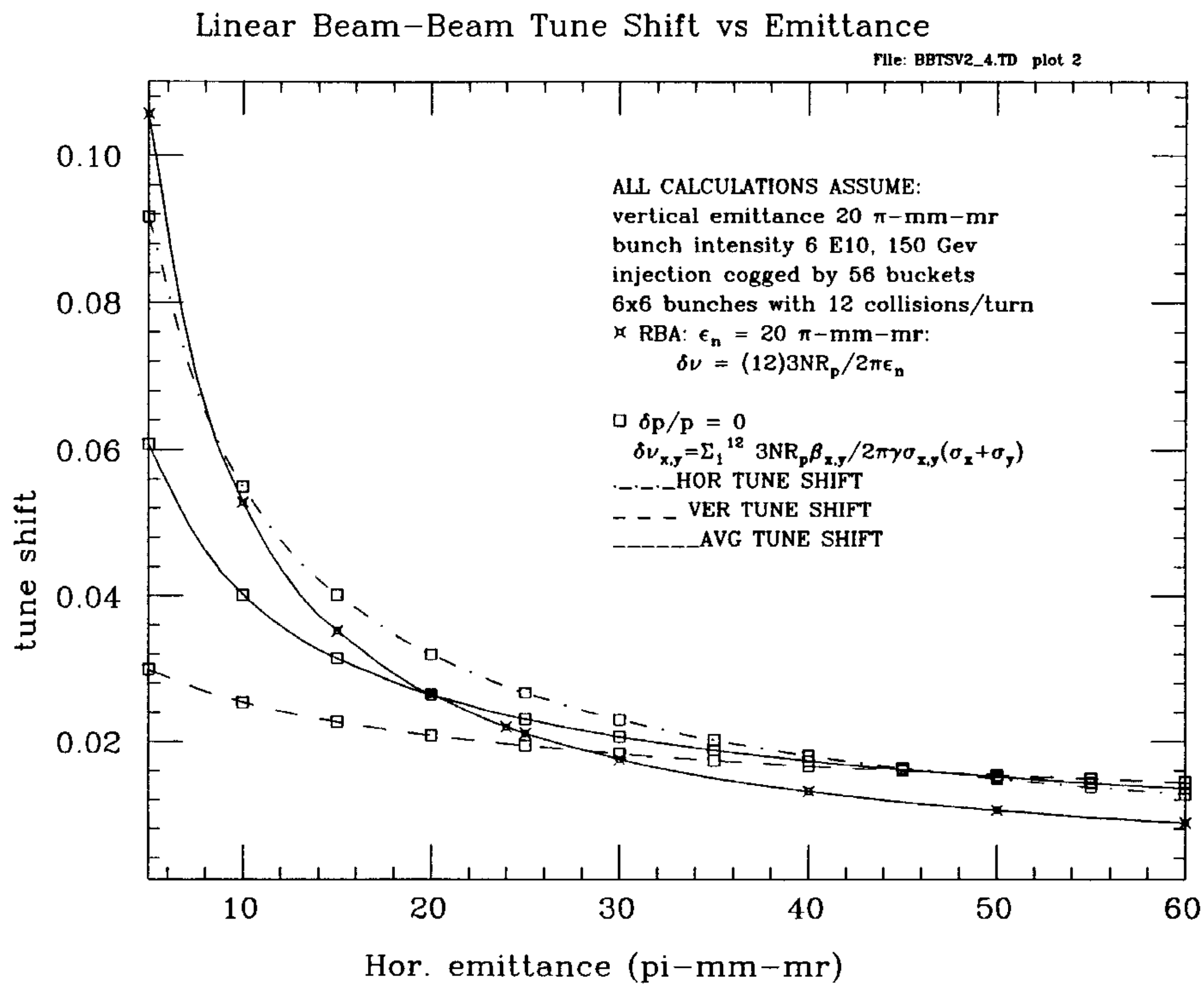
Linear Beam–Beam Tune Shift vs Emittance
File: BBTSV2_4.TD plot 2
ALL CALCULATIONS ASSUME:
vertical emittance 20 π–mm–mr
bunch intensity 6 E10, 150 Gev
injection cogged by 56 buckets
6x6 bunches with 12 collisions/turn
RBA: ϵ_n = 20 π–mm–mr:
$\delta\nu = (12)3NR_p/2\pi\epsilon_n$
$\delta p/p = 0$
$\delta\nu_{x,y}=\Sigma_1^{12}\ 3NR_p\beta_{x,y}/2\pi\gamma\sigma_{x,y}(\sigma_x+\sigma_y)$
HOR TUNE SHIFT
VER TUNE SHIFT
AVG TUNE SHIFT
tune shift
0.10
0.08
0.06
0.04
0.02
10
20
30
40
50
60
Hor. emittance (pi–mm–mr)

FIGURE 6

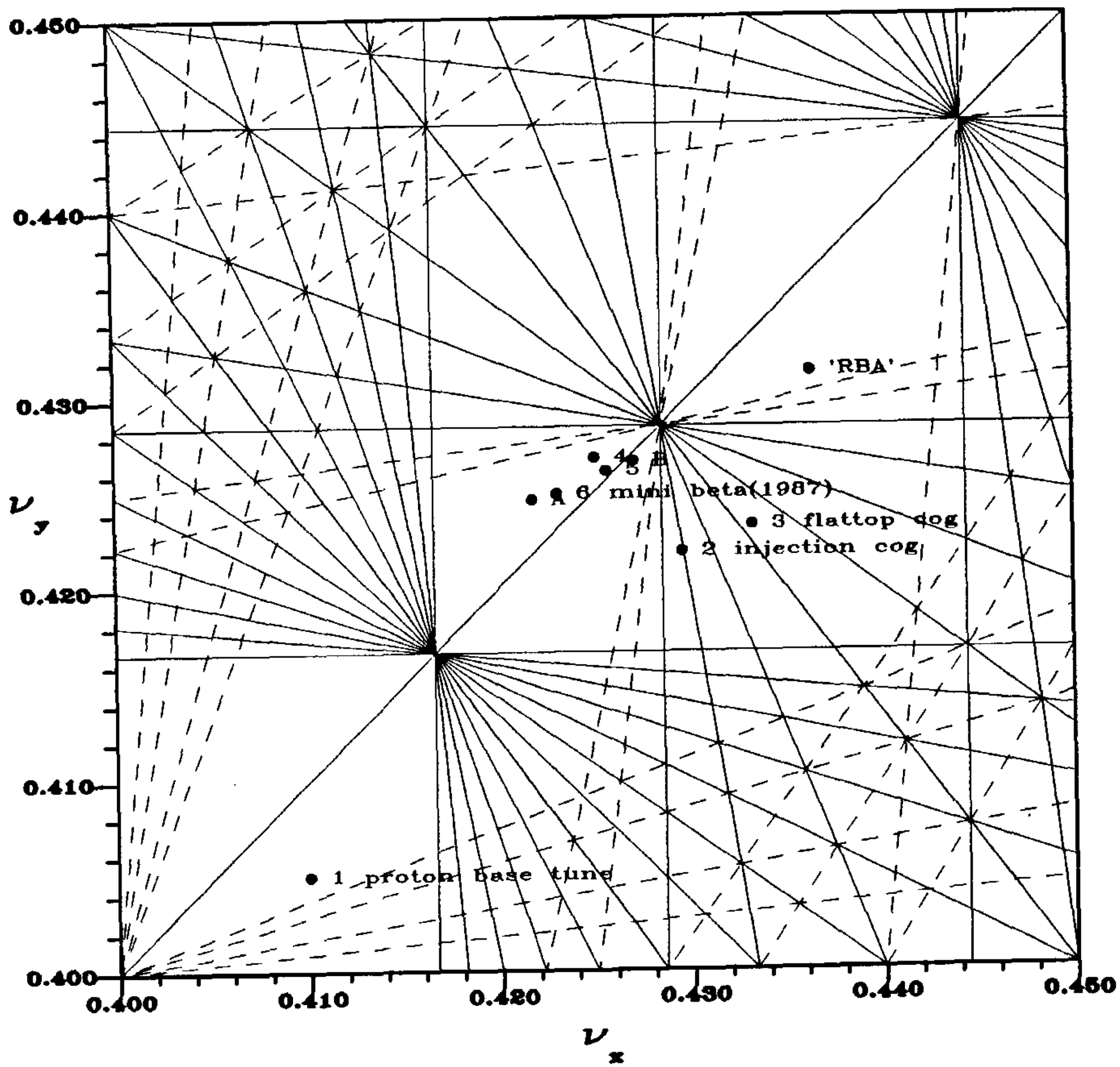

0.450
0.440
0.430
0.420
0.410
0.400
ν_y
ν_x
'RBA'
4
5
B
A
6 mini beta(1987)
3 flattop dog
2 injection cog
1 proton base tune

FIGURE 7

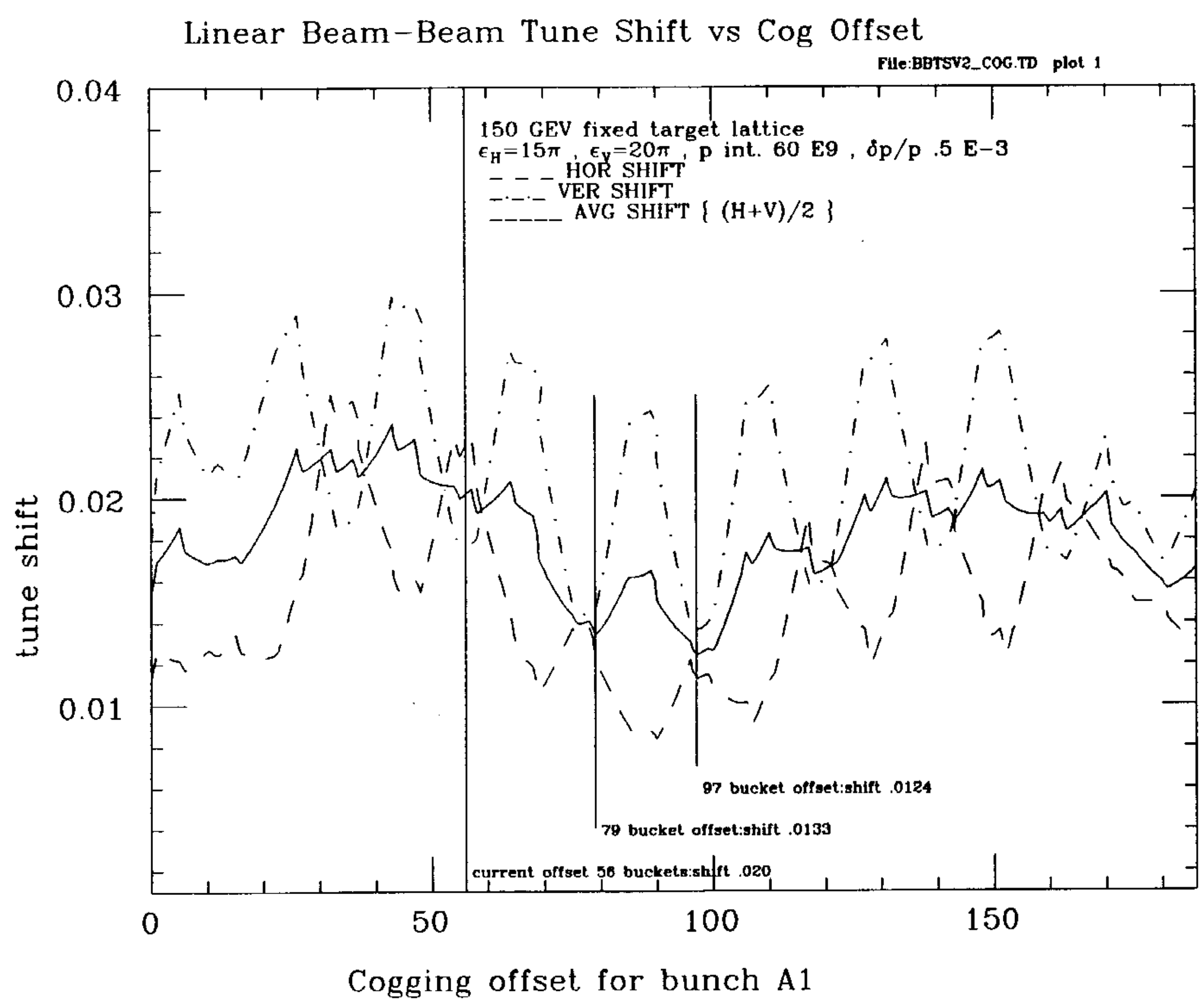

Linear Beam-Beam Tune Shift vs Cog Offset
File:BBTSV2_COG.TD plot 1
150 GEV fixed target lattice
$\epsilon_H=15\pi$, $\epsilon_V=20\pi$, p int. 60 E9 , $\delta p/p$ .5 E-3
HOR SHIFT
VER SHIFT
AVG SHIFT { (H+V)/2 }
97 bucket offset:shift .0124
79 bucket offset:shift .0133
current offset 56 buckets:shift .020
0.04
0.03
0.02
0.01
tune shift
0
50
100
150
Cogging offset for bunch A1

FIGURE 8

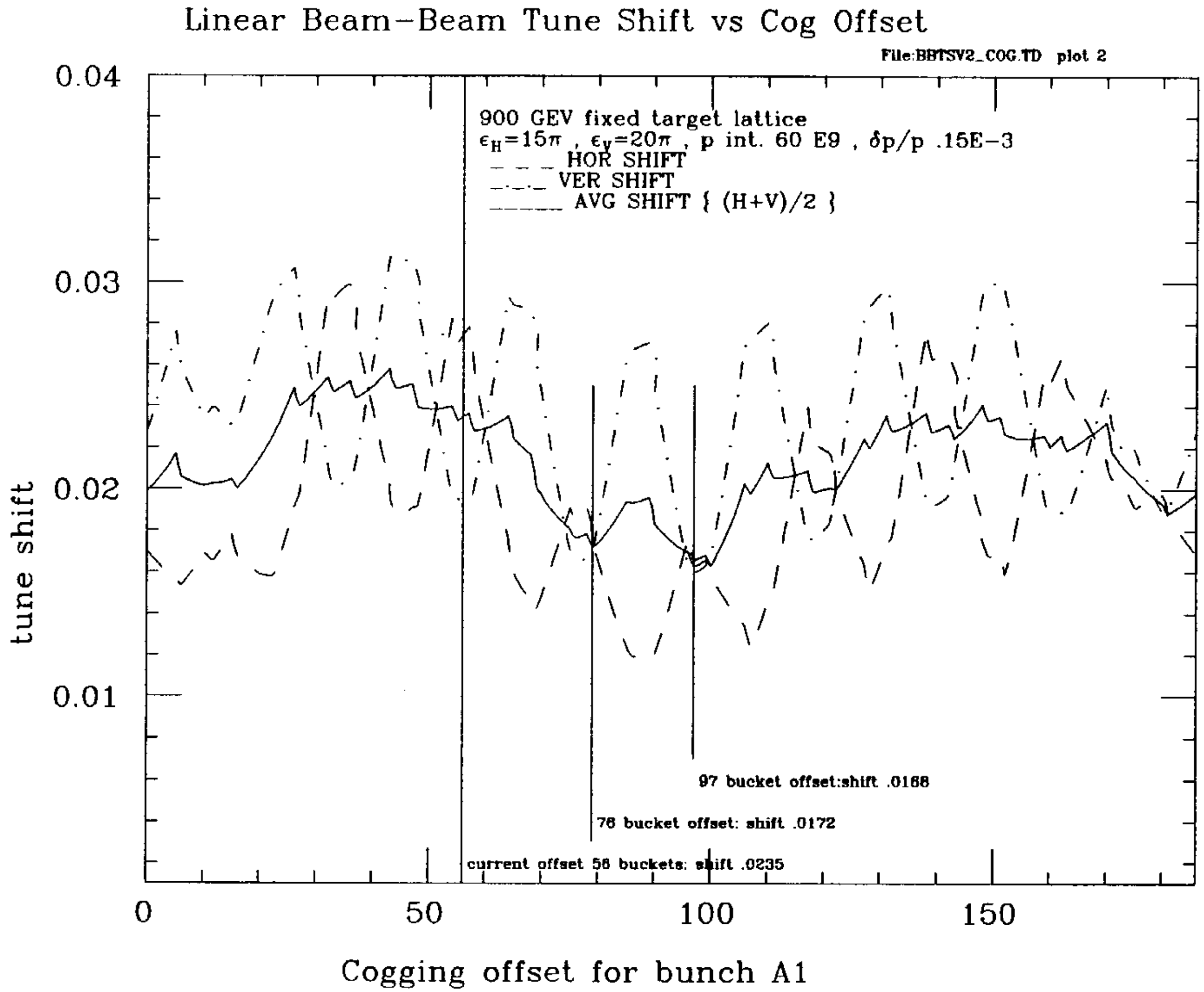
Linear Beam-Beam Tune Shift vs Cog Offset
File:BBTSV2_COG.TD plot 2
900 GEV fixed target lattice
ϵ_H=15π , ϵ_V=20π , p int. 60 E9 , δp/p .15E-3
HOR SHIFT
VER SHIFT
AVG SHIFT { (H+V)/2 }
97 bucket offset:shift .0168
76 bucket offset: shift .0172
current offset 56 buckets: shift .0235
0.04
0.03
0.02
0.01
tune shift
0
50
100
150
Cogging offset for bunch A1

FIGURE 9

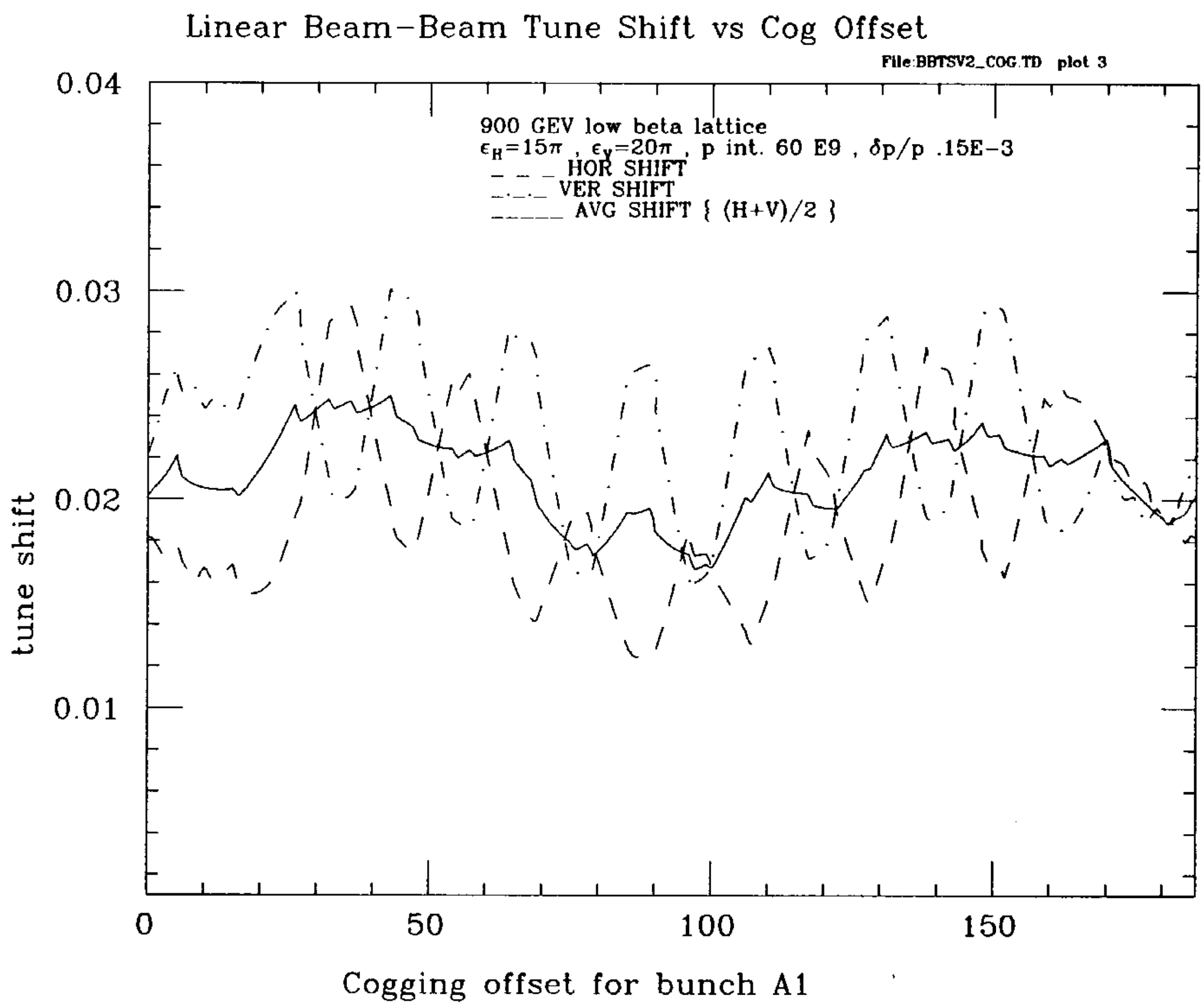
Linear Beam−Beam Tune Shift vs Cog Offset
File:BBTSV2_COG.TD plot 3
900 GEV low beta lattice
ϵ_H=15π , ϵ_V=20π , p int. 60 E9 , δp/p .15E−3
HOR SHIFT
VER SHIFT
AVG SHIFT { (H+V)/2 }
0.04
0.03
0.02
0.01
tune shift
0
50
100
150
Cogging offset for bunch A1

FIGURE 10

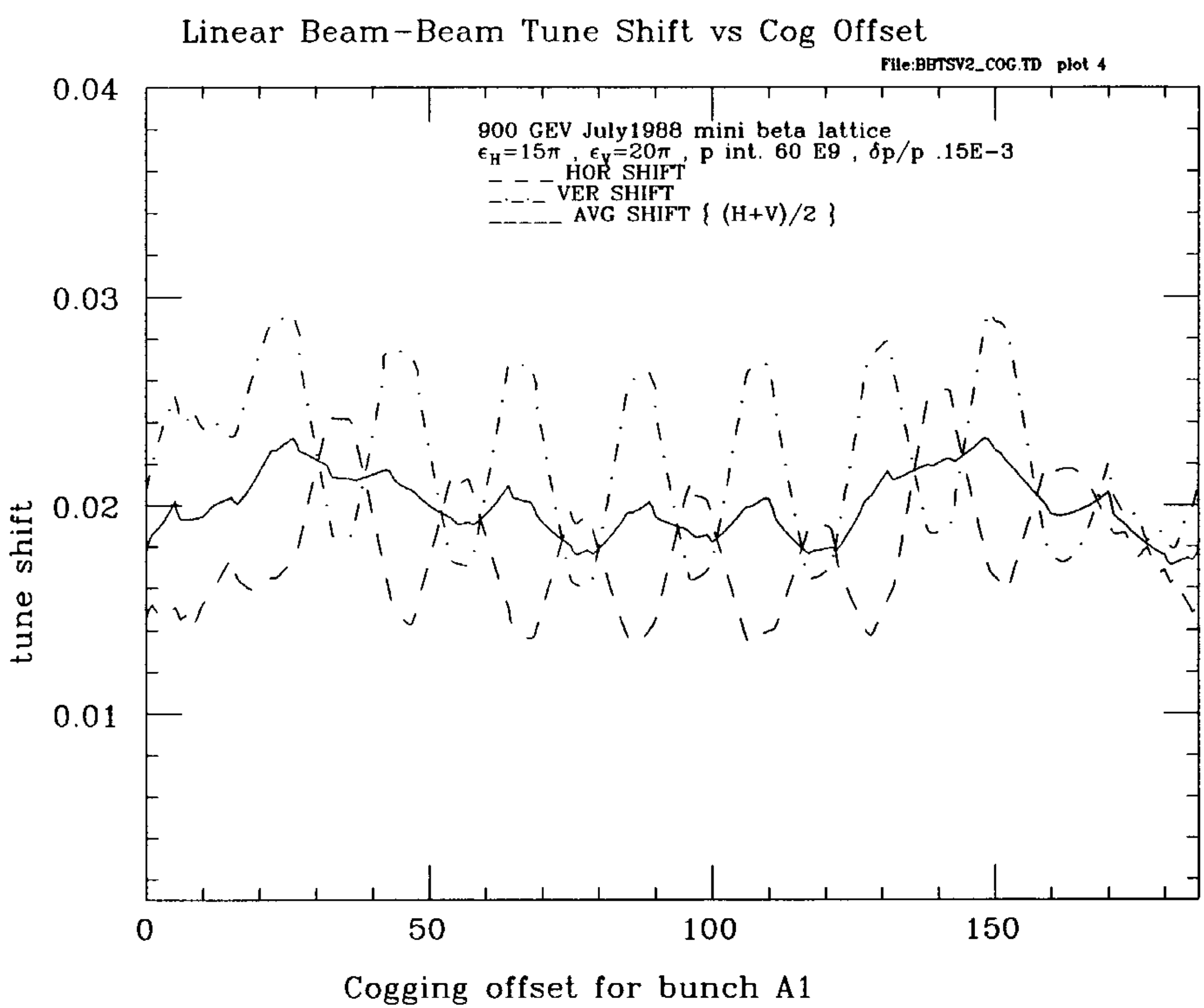
Linear Beam-Beam Tune Shift vs Cog Offset
File:BBTSV2_COG.TD plot 4
900 GEV July1988 mini beta lattice
$\epsilon_H=15\pi$, $\epsilon_V=20\pi$, p int. 60 E9 , $\delta p/p$ .15E-3
HOR SHIFT
VER SHIFT
AVG SHIFT { (H+V)/2 }
0.04
0.03
0.02
0.01
tune shift
0
50
100
150
Cogging offset for bunch A1

FIGURE 11

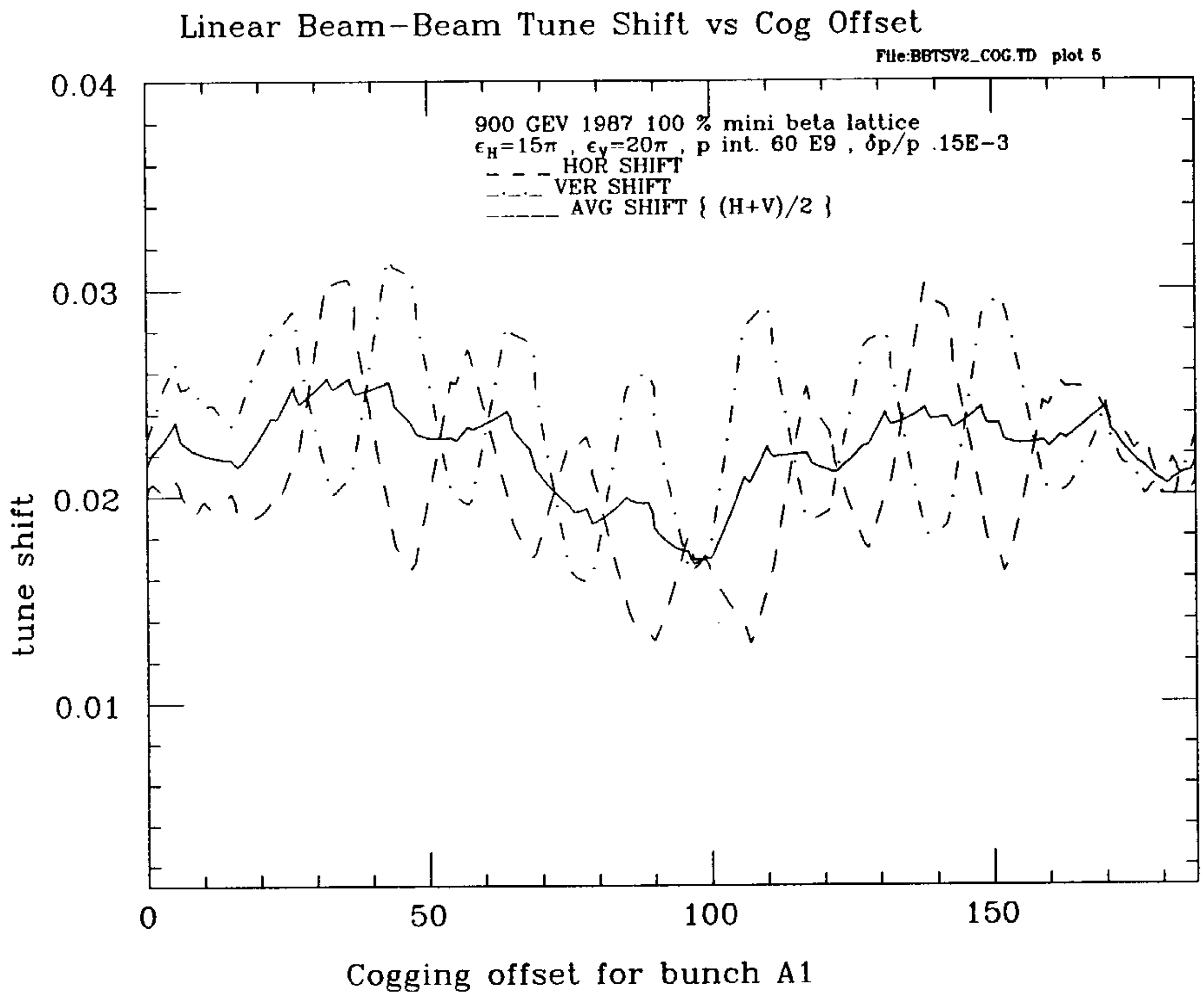
Linear Beam-Beam Tune Shift vs Cog Offset
File:BBTSV2_COG.TD plot 5
900 GEV 1987 100 % mini beta lattice
ϵ_H=15π , ϵ_V=20π , p int. 60 E9 , δp/p .15E-3
HOR SHIFT
VER SHIFT
AVG SHIFT { (H+V)/2 }
0.04
0.03
0.02
0.01
tune shift
0
50
100
150
Cogging offset for bunch A1

FIGURE 12

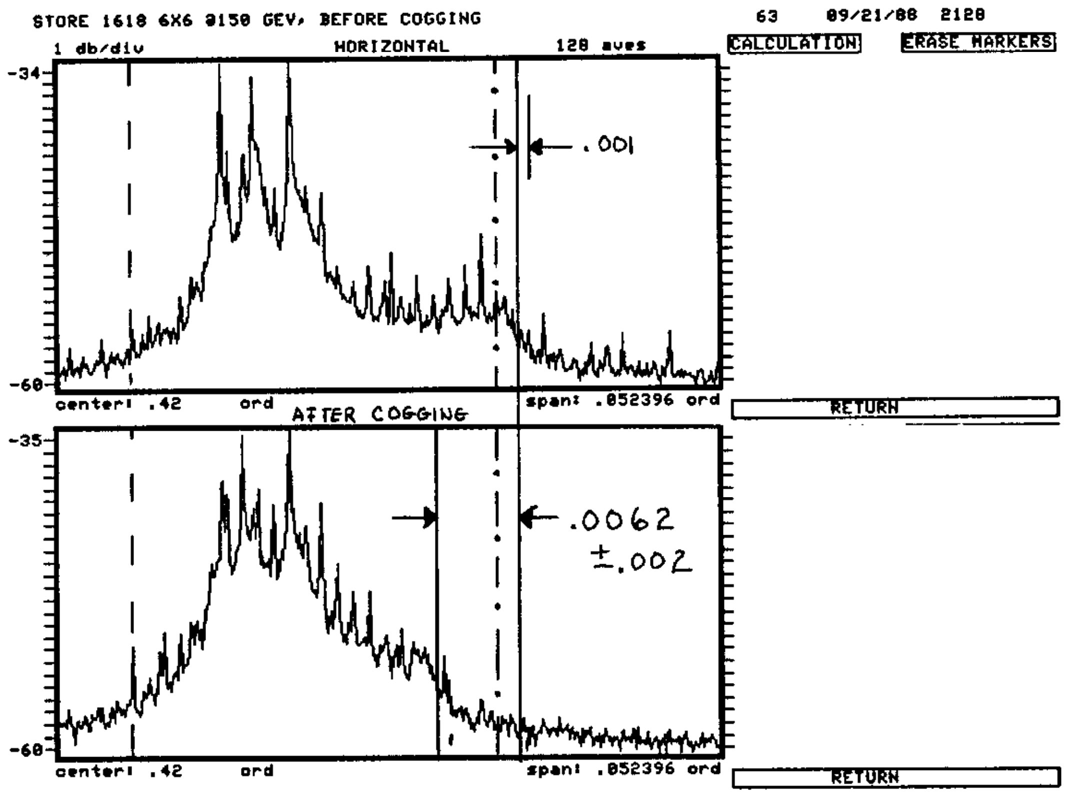

FIGURE 13A

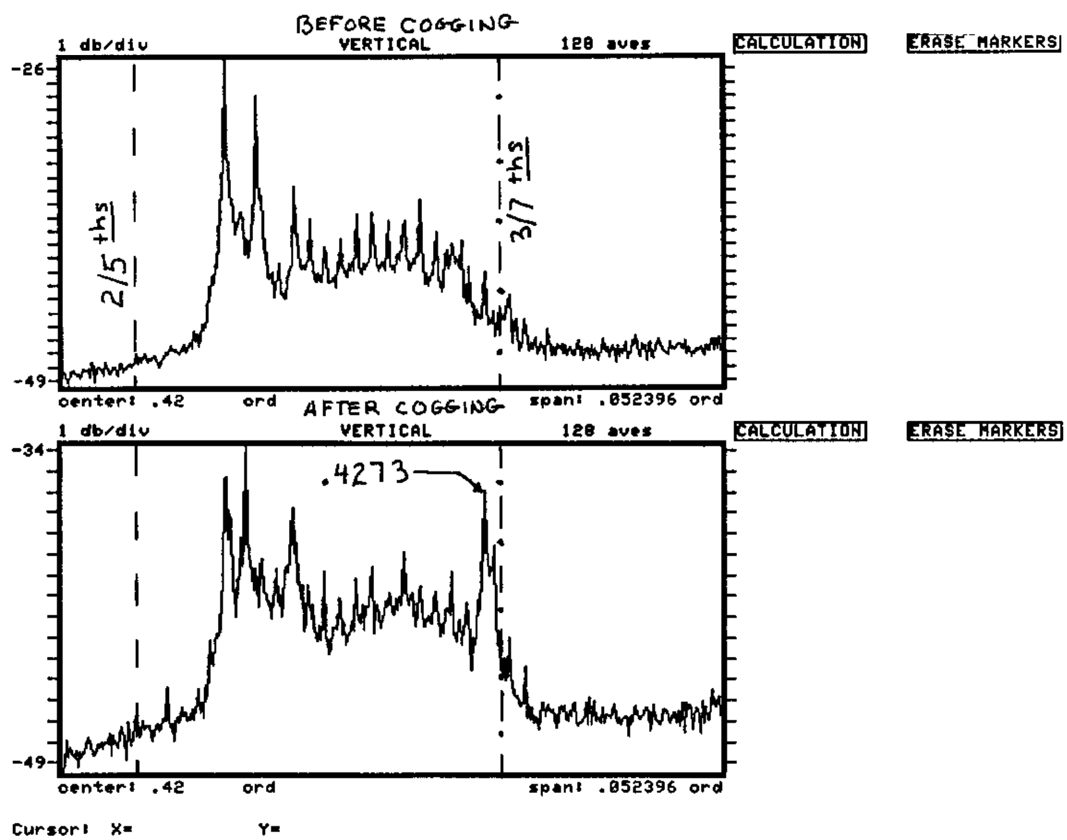

FIGURE 13B